arXiv:2007.00748v1 [cs.CV] 1 Jul 2020

Weakly-Supervised Segmentation for Disease Localization in Chest X-Ray Images

Ostap Viniavskyi*[1], Mariia Dobko*[1,2], and Oles Dobosevych[1]

[1] The Machine Learning Lab at Ukrainian Catholic University, Lviv, Ukraine
{viniavskyi,dobko_m,dobosevych}@ucu.edu.ua
[2] SoftServe, Ukraine
{mdobk}@softserveinc.com

Abstract. Deep Convolutional Neural Networks have proven effective in solving the task of semantic segmentation. However, their efficiency heavily relies on the pixel-level annotations that are expensive to get and often require domain expertise, especially in medical imaging. Weakly supervised semantic segmentation helps to overcome these issues and also provides explainable deep learning models.

In this paper, we propose a novel approach to the semantic segmentation of medical chest X-ray images with only image-level class labels as supervision. We improve the disease localization accuracy by combining three approaches as consecutive steps. First, we generate pseudo segmentation labels of abnormal regions in the training images through a supervised classification model enhanced with a regularization procedure. The obtained activation maps are then post-processed and propagated into a second classification modelInter-pixel Relation Network, which improves the boundaries between different object classes. Finally, the resulting pseudo-labels are used to train a proposed fully supervised segmentation model.

We analyze the robustness of the presented method and test its performance on two distinct datasets: PASCAL VOC 2012 and SIIM-ACR Pneumothorax. We achieve significant results in the segmentation on both datasets using only image-level annotations. We show that this approach is applicable to chest X-rays for detecting an anomalous volume of air in the pleural space between the lung and the chest wall. Our code has been made publicly available[3].

Keywords: Weakly-supervised learning · Segmentation · Deep Learning · Chest X-rays · Disease localization · Explainable models

1 Introduction

Applications of Convolutional Neural Networks to medical images have recently produced efficient solutions for a vast variety of medical problems, such as segmentation of lung nodules in computed tomography (CT) scans [13], lesions

*These authors contributed equally to the work
[3]Implementation is available at https://github.com/ucuapps/WSMIS

detection in mammography images [1], segmentation of brain gliomas from MRI images [4] and others [26,30]. One of the greatest challenges for using deep learning methods in medicine is the lack of large annotated datasets, especially with pixel-level labeled data. Creating such datasets is often very expensive and time consuming. For instance, Lin et al. [20] calculated that collecting bounding boxes for each class is about 15 times faster than producing a ground-truth pixel-wise segmentation mask; getting image-level labels is even easier. Moreover, domain expertise is required to label medical data, which poses another challenge as the doctor's time is costly and could more effectively be used for a patient's diagnosis and disease treatment. Working with image-level annotations also decreases the probability of disagreement between experts, since pixel-wise annotations tend to have more noise and vary among labelers.

To decrease the resources spent on labeling while preserving its quality, we propose a novel weakly-supervised approach to image segmentation that uses only image-level labels. Our method is domain-independent; we have tested it on several distant datasets, including popular PASCAL VOC 2012 [11], and a medical dataset, SIIM-ACR Pneumothorax [28]. We achieve 64.6 mean intersection-over union (mIoU) score on PASCAL VOC 2012 [11] validation set. Our method is capable of segmenting medical images with limited supervision achieving 76.77 mIoU score on the test set of SIIM-ACR Pneumothorax dataset [28]. The automatic approach to finding Pneumothorax could be used to triage chest radiographs requiring priority interpretation, to rapidly identify critical cases, and also provide a second-opinion for radiologists to make a more confident disease diagnosis.

2 Related Work

The objective of weakly-supervised segmentation is to create models capable of pixel-wise segmentation based on image-level labels. The existing approaches can be categorized by their methodologies into four groups: Expectation-Maximization, Multiple Instance Learning, Self-Supervised Learning, and Object Proposal Class Inference [6]. In this paper, we follow the self-supervised paradigm, which suggests training a fully supervised segmentation model on the created pseudo-pixel-level annotations, also known as Class Activation Maps (CAM) [33], which are extracted from the classification network. This paradigm is the most challenging one as it leads to the least informative form of weak supervision providing no location information for the objects. However, judging from the quantitative performance on PASCAL VOC 2012 [11] validation set, the top five methods of weakly-supervised segmentation use the self-supervised learning approach [6].

Many methods of self-supervised learning for semantic segmentation have been recently suggested. Kolesnikov et al. [18] propose Seed Expand Constrain (SEC) method, which trains a CNN, applies CAM to produce pseudo-ground-truth segments, and then trains a Fully Convolutional Network (FCN) optimizing three losses: one for the generated seeds, another for the image-level label, and, finally, a constraint loss against the maps processed by Conditional Ran-

dom Fields (CRF). Huang et al. [16] introduce Deep Seeded Region Growing (DSRG), which propagates class activations from high-confidence regions to adjacent regions with a similar visual appearance by applying a region-growing algorithm on the generated CAM. Lee et al. [19] present FickleNet, which trains a CNN at the image level with a regularization step represented as a center-fixed spatial dropout in the later convolutional layers, and then runs Grad-CAM [27] multiple times to generate a thresholded pseudo-labels for a segmentation step. Another approach, proposed by Ahn et al. [3], suggests using IRNet [3], which takes the random walk from low-displacement field centroids in the CAM up until the class boundaries as the pseudo-ground-truths for training an FCN. Ahn et al. [3] focus on the segmentation of the individual instances estimating two types of features in addition to CAM: a class-agnostic instance map and pairwise semantic affinities.

The weakly-supervised semantic segmentation on medical datasets has been explored in [22,2,10,5,25]. On the other hand, Ouyang et al. [23] combine the weakly-annotated data with well-annotated cases to segment Pneumothorax in chest X-rays. In our approach, we do not use any form of supervision besides image-level labels. We focus on developing a standardized method, which is efficient for various data types, especially for medical images.

3 Methodology

Our method can be split into three consecutive steps: Class Activation Maps generation, map enhancement with Inter-pixel Relation Network, and segmentation. After each step, we also add one or more post-processing techniques such as CRF, thresholding, noise filtering (small regions with low confidence).

Step 1. CAM generation First, we train fully-supervised classification models on image-level labels. The two tested architectures for this step were ResNet50 [14] and VGG16 [29] with additional three convolutional layers followed by ReLU activation. We also replace stride with dilation [32] in the last convolutional layers to increase the size of the final feature map while decreasing the output stride from 32 to 8. We improve the classification performance by including a regularization term, inspired by FickleNet [19]. For this, we use DropBlock [12]—a dropout technique, which to our best knowledge has not been tried in previous works on weakly-supervised segmentation. The trained models are then used to retrieve activation maps by applying the Grad-CAM++ [7] method. The resulting maps serve as pseudo labels for segmentation task.

Step 2. IRNet On the second step, IRNet [3] takes the generated CAM and trains two output branches that predict a displacement vector field and a class boundary map, correspondingly. They take feature maps from all the five levels of the same shared ResNet50 [14] backbone. The main advantage of IRNet [3] is its ability to improve boundaries between different object classes. We train it

on the generated maps, thus no extra supervision is required. This step allows us to obtain better pseudo-labels before proceeding to segmentation. To our best knowledge, this approach has not been used in the medical imaging domain before.

Step 3. Segmentation For the segmentation step, we train DeepLabv3+ [9] and U-Net [26] models with different backbones, which have proven to produce reliable results in fully supervised semantic segmentation on medical images [30,26]. The used backbones include ResNet50 [14] and SEResNeXt50 [15]. We modify the binary cross-entropy (BCE) loss during segmentation by adding weights to a positive class to prevent overfitting towards normal cases.

4 Experiments and Results

4.1 Reproducibility

PyTorch [24] was used for implementing and training all steps of our approach: extracting localization maps via the classification networks, improving obtained maps with IRNet [3] and segmenting the image during segmentation task. All the experiments were performed on four Nvidia Tesla K80 GPUs.

4.2 Datasets and evaluation metric

We conduct experiments on two datasets: PASCAL VOC 2012 [11] and SIIM-ACR Pneumothorax [28]. We evaluate the quality of our pseudo-ground-truth and the performance of the segmentation model trained on them using mIoU.

PASCAL VOC 2012 [11] is an image segmentation benchmark dataset containing 20 object classes, and a background class. As in other works on weakly-supervised segmentation, we train our models using augmented 10,582 training images with image-level labels. We report mIoU for 1,449 validation images.

SIIM-ACR Pneumothorax [28] is a competition that provides an open dataset of chest X-ray images with pixel-wise annotation for regions affected by Pneumothorax: a collapsed lung, where an abnormal volume of air is formed in the pleural space between the lung and the chest wall. This dataset was formed from a subset of ChestX-ray14 dataset [31], but relabeled by professional radiologists, and additionally annotated on a pixel level. The specified competition has two stages; ground truth labels are provided only for the first, the second is evaluated on the competition website. Thus, we divided images from the first stage into three sets: train, validation and test. Totally, 12,047 frontal-view chest X-ray cases are in the dataset. We use 2,379 positive and 8,296 negative images for training, 145 and 541 for validation, 145 and 541 for the test.

4.3 Data challenges

SIIM-ACR Pneumothorax [28] dataset has a severe class imbalance problem. The number of normal cases exceeds approximately 4 times the number of positive

ones. In order to prevent overfitting towards healthy patients we use various augmentation techniques such as scaling, rotation, blur, brightness adjustment, and horizontal flipping. We also add sampling in our data loader during training, which selects the constant ratio between negative and positive class. Another challenge in this dataset is the size of regions of interest. Pneumothorax usually affects a very small area of lungs resulting in a high disbalance among the image pixels. We solve this problem by adding weights for positive class to binary cross-entropy loss. Due to these data challenges we evaluate the performance of our method on SIIM-ACR Pneumothorax not only for all images in validation and test sets, but also separately for positive cases, see Table 3.

4.4 Experiments

Step 1. CAM generation For classification we implement ResNet50, and VGG16. As suggested in previous work [17], we added three convolutional layers on the top of the fully-convolutional backbone, each of which is followed by a ReLU. The conducted experiments show that adding DropBlock regularization to our classification models improves their performance, see Table 1. For both datasets, the best classification results were achieved using VGG16, which was, thus, selected as the final model for this task. We test two methods for generating pseudo-annotations: Grad-CAM [27], and Grad-CAM++ [7]. Our experiments show that Grad-CAM++ [7], which utilizes a regularization that Grad-CAM is lacking of, provides better object localization through visual explanations of model predictions; cf. Table 2.

Step 2. IRNet For both datasets as post-processing of maps produced at Step 1, we use thresholding and then refine the pseudo-maps by dense CRF to better capture object shapes. The resulting annotations are used to train IRNet.

Step 3. Segmentation The obtained maps after IRNet step are used as the pseudo-labels for segmentation. We implement three networks to complete this

Table 1: Influence of DropBlock on PASCAL VOC 2012. Comparison of the classification model trained without regularization to a model with DropBlock.

Model	Multilabel F1-score (%)
ResNet50	88.08
ResNet50 with DropBlock regularization	88.2

Table 2: Comparison of CAM generation techniques on PASCAL VOC 2012.

Classification model	CAM extraction method	mIoU train	mIoU val
VGG16	Cam-Grad	0.4137	0.3511
VGG16	Cam-Grad++	**0.4176**	**0.3941**

task: U-Net [26], DeepLabv3 [8], and DeepLabv3+ [9]. We report results on PASCAL VOC 2012 produced by DeepLabv3+, as it shows better performance than DeepLabv3 with the same ResNet50 backbone. For SIIM-ACR Pneumothorax, however, U-Net with SEResNeXt50 [15] backbone shows the best results.

4.5 Training and optimization

For all the models, three optimization methods are examined: SGD, Adam and RAdam [21]. For Pneumothorax segmentation, SGD optimizer is applied with the learning rate initiated as 6e-5 and gradually decreasing each epoch, whereas momentum is set to 0.9, and weight decay to 1e-6. The size of network inputs is 512x512, the batch is 48, and it is balanced according to class distribution using augmentations to increase the sample of positive cases.

4.6 Results

The comparison of segmentation methods using the same chest X-ray datasets is not simple due to the challenge of finding public medical data. Moreover, this work is the first to present the results of weakly-supervised segmentation methods on SIIM-ACR Pneumothorax [28] data. However, the performance of our models is comparable to Ouyang et al. [23], who reported their scores on a collected closed dataset of Pneumothorax. These authors train their method with different combinations of well- and weakly-annotated data, whereas our method uses only image-level labels. In Table 3 we show how the results improve with each step of our approach; the result of Ouyang et al. [23] model trained on 400 weakly-annotated and 400 well-annotated cases is specified too.

Table 3: Results on SIIM-ACR Pneumothorax validation and test sets after each step of our method. Calculated for only positive cases (pos.), and for the whole set, including the healthy patients (all). The Ouyang et al. method, whose result is demonstrated, was trained on 400 weakly-annotated and 400 well-annotated cases.

		mIoU val		mIoU test	
Dataset	Method	pos.	all	pos.	all
SIIM-ACR Pneum. [28]	Step 1. CAM	0.117	0.7633	0.142	0.7590
SIIM-ACR Pneum. [28]	Step 2. IRNet	0.122	0.7645	0.154	0.7607
SIIM-ACR Pneum. [28]	Step 3. Segm.	0.148	0.7649	0.162	0.7677
Custom [23]	Ouyang et al.[23]	-	-	-	0.669

We present method's explainability via disease localization regions; cf. Figure 1. We provide qualitative results of segmentation on validation images from both datasets in Figure 2 and Figure 3. We show the resulting maps at each step of our method; the figures demonstrate how the performance improves after each step.

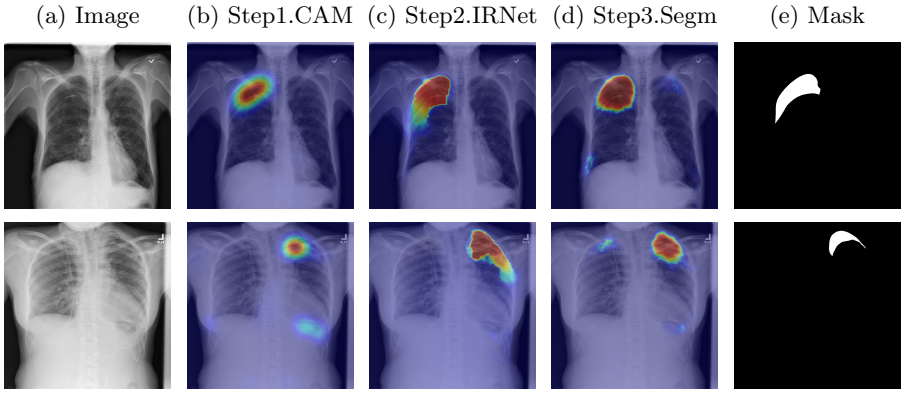


Fig. 1: Pneumothorax localization maps for (a) a random image from the test set at each consecutive step of our method: (b) map after CAM extraction, (c) improved map by IRNet trained on the outcomed of step 1, (d) prediction of U-Net trained on step 2 results, all compared to (e) ground truth mask.

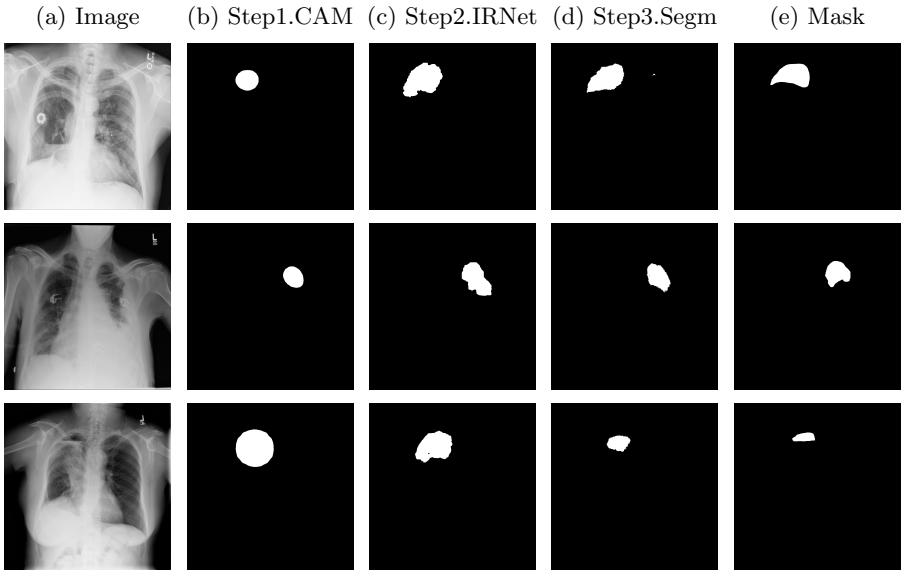


Fig. 2: Segmentation predictions for (a) a random image from test set of SIIM-ACR Pneumothorax produced at each step of our approach: (b) CAM extraction, (c) IRNet, (d) U-Net segmentation, compared to (e) ground truth mask.

We achieve comparable results to state-of-the-art method on PASCAL VOC 2012; cf. Table 4.

We evaluate our method on the second stage test set on the competition server [28] to compare it against a fully-supervised upper-performance limit. We

achieve 0.769 Dice score while the first place solution got 0.868 using pixel-level labels for training. Our method proves the capability of using only image-level annotations for semantic segmentation on chest X-rays, nevertheless, attaining as good or even better results than those produced by fully supervised networks is still a challenge for weakly-supervised approaches.

Table 4: Comparison of weakly-supervised semantic segmentation methods on PASCAL VOC 2012 validation set. Our approach is evaluated after each of the proposed steps, where each step is trained on the outcomes of the previous one.

Method	Year	mIoU
Our method. Step 1. CAM	2020	0.479
Our method. Step 2. IRNet	2020	0.631
Our method. Step 3. Segmentation	2020	**0.646**
IRNet [3]	2019	0.635
FickleNet [19]	2019	**0.649**
DSRG (ResNet101) [16]	2018	0.614
SEC [18]	2016	0.507

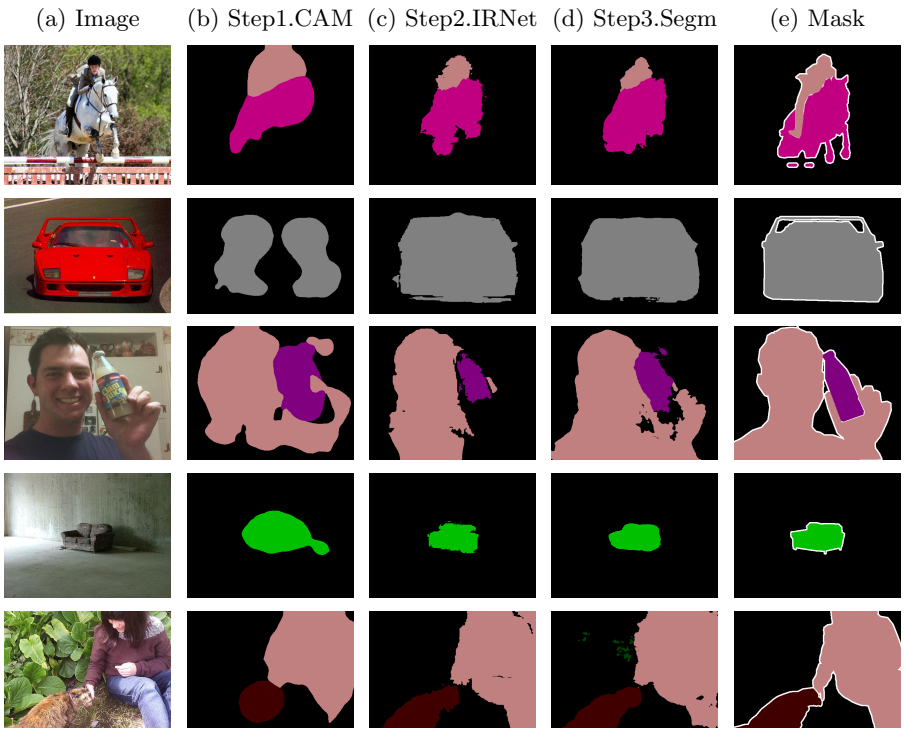


Fig. 3: Visualization of segmentation predictions on PASCAL VOC 2012 for (a) an image produced at each step of our approach: (b) CAM extraction, (c) IRNet, (d) DeepLabv3+ segmentation, compared to (e) ground truth mask.

5 Clinical Relevance

During diagnosing procedure the final decision maker is a doctor, while AI-powered decision support systems can assist by detecting regions of interest and presenting the data in a convenient format that doctors can use. With an automatic image segmentation solution, the healthcare provider can reach higher efficiency by saving doctors' time spent on the primary analysis of images. At the same time it will increase diagnosis accuracy by providing the second opinion. The major problem in building such a solution is the lack of large amounts of pixel-wise labeled data that are extremely costly in terms of the expert time required for their annotation. With our approach, which requires only image-level annotations, the costs can be reduced dramatically. In the long run, it allows the cheaper implementation of segmentation models, also facilitating research in the area by overcoming the problem of collecting datasets with pixel-wise annotations. Saving doctors' time on diagnosis is especially important during the disease widespread such as COVID-19, when large number of people are affected by a disease and the amount of required screening procedures grows exponentially.

Using our method for medical images can automate parts of the radiology workflow cutting operational costs for the hospitals. The proposed approach was designed to be general and applicable to other medical purposes; for example detection of various thoracic diseases.

6 Conclusions

We present a novel method of weakly-supervised semantic segmentation that demonstrated its efficiency for detecting anomalous regions on chest X-ray images. In particular, we propose a three-step approach to weakly-supervised semantic segmentation, which uses only image-level labels as supervision. Next, we customize and expand the previous works by including supplementary steps such as regularization, IRNet, and various post-processing techniques. Also, the method is general, domain independent and explainable via localization maps at each step. We evaluated it on two datasets of different nature; however, it can also be implemented in other medical problems.

Acknowledgements

This research was supported by SoftServe and Faculty of Applied Sciences at Ukrainian Catholic University (UCU), whose collaboration allowed to create SoftServe Research Group at UCU. The authors thank Rostyslav Hryniv for helpful and valuable feedback.

References

1. Abdelhafiz, D., Yang, C., Ammar, R., Nabavi, S.: Deep convolutional neural networks for mammography: advances, challenges and applications. BMC bioinformatics **20**(11), 281 (2019)
2. Agarwal, V., Tang, Y., Xiao, J., Summers, R.M.: Weakly supervised lesion co-segmentation on CT scans. arXiv preprint arXiv:2001.09174 (2020)
3. Ahn, J., Cho, S., Kwak, S.: Weakly supervised learning of instance segmentation with inter-pixel relations. In: Proceedings of the IEEE Conference on Computer Vision and Pattern Recognition. pp. 2209–2218 (2019)
4. Archa, S., Kumar, C.S.: Segmentation of brain tumor in MRI images using CNN with edge detection. In: 2018 International Conference on Emerging Trends and Innovations in Engineering and Technological Research (ICETIETR). pp. 1–4. IEEE (2018)
5. Cai, J., Tang, Y., Lu, L., Harrison, A.P., Yan, K., Xiao, J., Yang, L., Summers, R.M.: Accurate weakly-supervised deep lesion segmentation using large-scale clinical annotations: Slice-propagated 3d mask generation from 2d recist. In: International Conference on Medical Image Computing and Computer-Assisted Intervention. pp. 396–404. Springer (2018)
6. Chan, L., Hosseini, M.S., Plataniotis, K.N.: A comprehensive analysis of weakly-supervised semantic segmentation in different image domains. arXiv preprint arXiv:1912.11186 (2019)
7. Chattopadhay, A., Sarkar, A., Howlader, P., Balasubramanian, V.N.: Grad-cam++: Generalized gradient-based visual explanations for deep convolutional networks. In: 2018 IEEE Winter Conference on Applications of Computer Vision (WACV). pp. 839–847. IEEE (2018)
8. Chen, L.C., Papandreou, G., Schroff, F., Adam, H.: Rethinking atrous convolution for semantic image segmentation. arXiv preprint arXiv:1706.05587 (2017)
9. Chen, L.C., Zhu, Y., Papandreou, G., Schroff, F., Adam, H.: Encoder-decoder with atrous separable convolution for semantic image segmentation. In: Proceedings of the European conference on computer vision (ECCV). pp. 801–818 (2018)
10. Demiray, B., Rackerseder, J., Bozhinoski, S., Navab, N.: Weakly-supervised white and grey matter segmentation in 3d brain ultrasound. arXiv preprint arXiv:1904.05191 (2019)
11. Everingham, M., Van Gool, L., Williams, C.K.I., Winn, J., Zisserman, A.: The PASCAL Visual Object Classes Challenge 2012 (VOC2012) Results. http://www.pascal-network.org/challenges/VOC/voc2012/workshop/index.html
12. Ghiasi, G., Lin, T.Y., Le, Q.V.: Dropblock: A regularization method for convolutional networks. In: Advances in Neural Information Processing Systems. pp. 10727–10737 (2018)
13. Gruetzemacher, R., Gupta, A., Paradice, D.: 3d deep learning for detecting pulmonary nodules in CT scans. Journal of the American Medical Informatics Association **25**(10), 1301–1310 (2018)
14. He, K., Zhang, X., Ren, S., Sun, J.: Deep residual learning for image recognition. In: Proceedings of the IEEE conference on computer vision and pattern recognition. pp. 770–778 (2016)
15. Hu, J., Shen, L., Sun, G.: Squeeze-and-excitation networks. In: Proceedings of the IEEE conference on computer vision and pattern recognition. pp. 7132–7141 (2018)
16. Huang, Z., Wang, X., Wang, J., Liu, W., Wang, J.: Weakly-supervised semantic segmentation network with deep seeded region growing. In: Proceedings of the

IEEE Conference on Computer Vision and Pattern Recognition. pp. 7014–7023 (2018)
17. Jiang, P.T., Hou, Q., Cao, Y., Cheng, M.M., Wei, Y., Xiong, H.K.: Integral object mining via online attention accumulation. In: Proceedings of the IEEE International Conference on Computer Vision. pp. 2070–2079 (2019)
18. Kolesnikov, A., Lampert, C.H.: Seed, expand and constrain: Three principles for weakly-supervised image segmentation. In: European Conference on Computer Vision. pp. 695–711. Springer (2016)
19. Lee, J., Kim, E., Lee, S., Lee, J., Yoon, S.: Ficklenet: Weakly and semi-supervised semantic image segmentation using stochastic inference. In: Proceedings of the IEEE conference on computer vision and pattern recognition. pp. 5267–5276 (2019)
20. Lin, T.Y., Maire, M., Belongie, S., Hays, J., Perona, P., Ramanan, D., Dollár, P., Zitnick, C.L.: Microsoft coco: Common objects in context. In: European conference on computer vision. pp. 740–755. Springer (2014)
21. Liu, L., Jiang, H., He, P., Chen, W., Liu, X., Gao, J., Han, J.: On the variance of the adaptive learning rate and beyond. arXiv preprint arXiv:1908.03265 (2019)
22. Lu, Z., Chen, D.: Weakly supervised and semi-supervised semantic segmentation for optic disc of fundus image. Symmetry **12**(1), 145 (2020)
23. Ouyang, X., Xue, Z., Zhan, Y., Zhou, X.S., Wang, Q., Zhou, Y., Wang, Q., Cheng, J.Z.: Weakly supervised segmentation framework with uncertainty: A study on pneumothorax segmentation in chest x-ray. In: International Conference on Medical Image Computing and Computer-Assisted Intervention. pp. 613–621. Springer (2019)
24. Paszke, A., Gross, S., Massa, F., Lerer, A., Bradbury, J., Chanan, G., Killeen, T., Lin, Z., Gimelshein, N., Antiga, L., Desmaison, A., Kopf, A., Yang, E., DeVito, Z., Raison, M., Tejani, A., Chilamkurthy, S., Steiner, B., Fang, L., Bai, J., Chintala, S.: Pytorch: An imperative style, high-performance deep learning library. In: Wallach, H., Larochelle, H., Beygelzimer, A., d Alch-Buc, F., Fox, E., Garnett, R. (eds.) Advances in Neural Information Processing Systems 32, pp. 8024–8035. Curran Associates, Inc. (2019), http://papers.neurips.cc/paper/9015-pytorch-an-imperative-style-high-performance-deep-learning-library.pdf
25. Qu, H., Wu, P., Huang, Q., Yi, J., Riedlinger, G.M., De, S., Metaxas, D.N.: Weakly supervised deep nuclei segmentation using points annotation in histopathology images. In: International Conference on Medical Imaging with Deep Learning. pp. 390–400 (2019)
26. Ronneberger, O., Fischer, P., Brox, T.: U-net: Convolutional networks for biomedical image segmentation. In: International Conference on Medical image computing and computer-assisted intervention. pp. 234–241. Springer (2015)
27. Selvaraju, R.R., Cogswell, M., Das, A., Vedantam, R., Parikh, D., Batra, D.: Grad-cam: Visual explanations from deep networks via gradient-based localization. In: Proceedings of the IEEE international conference on computer vision. pp. 618–626 (2017)
28. SIIM-ACR Pneumothorax Segmentation, https://www.kaggle.com/c/siim-acr-pneumothorax-segmentation
29. Simonyan, K., Zisserman, A.: Very deep convolutional networks for large-scale image recognition. arXiv preprint arXiv:1409.1556 (2014)
30. Skourt, B.A., El Hassani, A., Majda, A.: Lung CT image segmentation using deep neural networks. Procedia Computer Science **127**, 109–113 (2018)
31. Wang, X., Peng, Y., Lu, L., Lu, Z., Bagheri, M., Summers, R.M.: Chestx-ray8: Hospital-scale chest x-ray database and benchmarks on weakly-supervised classi-

fication and localization of common thorax diseases. In: Proceedings of the IEEE conference on computer vision and pattern recognition. pp. 2097–2106 (2017)
32. Yu, F., Koltun, V.: Multi-scale context aggregation by dilated convolutions. arXiv preprint arXiv:1511.07122 (2015)
33. Zhou, B., Khosla, A., Lapedriza, A., Oliva, A., Torralba, A.: Learning deep features for discriminative localization. In: Proceedings of the IEEE conference on computer vision and pattern recognition. pp. 2921–2929 (2016)

A Appendix

For the evaluation we use $mIoU$ (mean intersection over union), Dice score and $F1$-score.

The mIoU metric was used to compare our result to already existing approaches. For all images and k classes is defined as follows:

$$mIoU = \frac{1}{k}\sum_{i=1}^{k}\frac{TP_{ii}}{\sum\limits_{j=1}^{k}FN_{ij} + \sum\limits_{j=1}^{k}FP_{ij} - TP_{ii}},$$

where TP, FP, FN are numbers of true positive, false positive and false negative pixels respectively.

The Dice score was used to compare our results of weakly-supervised model to the first place solution with fully-supervised approach on SIIM-ACR Pneumothorax [28]. The metric is defined as follows:

$$Dice = \frac{2 \times TP}{(TP + FP) + (TP + FN)}$$

where TP, FP, FN are numbers of true positive, false positive and false negative pixels respectively. If all pixels are true negative, prediction is considered correct and metric equals 1.

The $F1$-score was used to compare approaches on a first step step of our pipeline — classification. The metric is defined as follows:

$$F1 = \frac{2 \times precision \times recall}{pression + recall}$$

where $precission = \frac{TP}{TP+FP}$, $recall = \frac{TP}{TP+FN}$, and TP, FP, FN are true positive, false positive and false negative rates respectively.